Fermionic transport through a driven quantum point contact: breakdown of Floquet thermalization beyond a critical driving frequency.

Ivan V. Dudinets

Russian Quantum Center, 30 Bolshoy Boulevard, building 1,
Skolkovo Innovation Center territory, Moscow, 121205, Russia and
Moscow Institute of Physics and Technology, Institutskii per. 9, Dolgoprudnyi, 141700, Russia

Oleg Lychkovskiy

Skolkovo Institute of Science and Technology, the territory of the Skolkovo Innovation Center,
Bolshoy Boulevard, 30, p.1, Moscow 121205, Russia and
Steklov Mathematical Institute of Russian Academy of Sciences, Gubkina str., 8, Moscow, 119991, Russia
(Dated: November 8, 2024)

We study a quantum system that consists of two fermionic chains coupled by a driven quantum point contact (QPC). The QPC contains a bond with a periodically varying tunneling amplitude. Initially the left chain is packed with fermions while the right one is empty. We numerically track the evolution of the system and demonstrate that, at frequencies above a critical one, the current through the QPC halts, and the particle imbalance between the chains remains forever. This implies a spectacular breakdown of the Floquet version of the eigenstate thermalization hypothesis which predicts a homogeneous particle density profile at large times. We confirm the effect for various driving protocols and interparticle interactions.

Introduction. Leveraging a rich phenomenology of quantum transport is essential for the advancement of science and technology at nano- and microscales. The unceasing theoretical efforts in understanding this phenomenology are of crucial importance, as they provide the foundation to interpret experimental results, predict new phenomena, and guide the design of next-generation quantum and microelectronic devices [1–5].

Here we contribute to these efforts by studying a system of two tight-binding fermionic chains connected by a quantum point contact (QPC) with a periodically driven tunneling amplitude, see Fig. 1. Initially, the left chain is filled by fermions while the right one is empty.

This system has been studied previously in the case of noninteracting fermions [6]. It has been shown to exhibit a nonequilibrium phase transition under the variation of the driving frequency: while for low frequencies the QPC is conducting, for frequencies above the single-particle band gap the QPC turns to be insulating, and the initial imbalance of particle densities lasts forever [6].

At first sight, the latter behavior should become impossible when the interactions between the fermions come into play. This expectation is based on the Floquet version of the eigenstate thermalization hypothesis (the Floquet ETH) [7, 8] which is believed to hold for generic interacting periodically-driven quantum many-body systems [7–13]. The Floquet ETH predicts that a state locally indistinguishable from the infinite-temperature thermal state will establish in the long run, which implies the homogeneous distribution of particles across both chains.

Here we demonstrate that this expectation is wrong: the QPC remains insulating above a critical frequency even when the interactions between the fermions are on.

This implies the breakdown of the Floquet ETH above the critical frequency.

The rest of the Letter is organized as follows. In the next section we introduce our model, observables and methods. Then we report and interpret the results. Finally, we discuss the results and give an outlook of possible further developments.

Model. The system under study consists of two one-dimensional chains harboring spinless fermions, see Fig. 1. The lengths of the chains are $(L + 1)$ and L. They are chosen to be unequal to avoid degeneracies due to the reflection symmetry. The chains are connected by a driven QPC. The total Hamiltonian reads

$$H_t = H_L + H_R + V_{\text{int}} + V_t, \qquad (1)$$

Here H_L and H_R describe hopping along left and right chains, respectively,

$$H_L = -\frac{1}{2} \sum_{j=1}^{L} (c_j^\dagger c_{j+1} + c_{j+1}^\dagger c_j), \qquad (2)$$

$$H_R = -\frac{1}{2} \sum_{j=L+2}^{2L} (c_j^\dagger c_{j+1} + c_{j+1}^\dagger c_j), \qquad (3)$$

c_j are fermionic annihilation operators, V_{int} is the interparticle interaction term and V_t is the time-periodic Hamiltonian of the QPC acting exclusively on the pair of boundary sites, see Fig 1. Here we focus on the specific
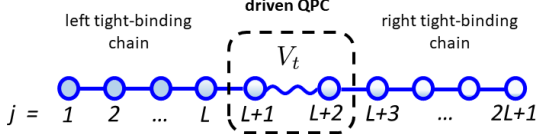
FIG. 1. The system under study consists of two fermionic tight-binding chains coupled by a bond with a periodically driven tunneling amplitude. The bond constitutes the time-dependent quantum point contact.

V_t and V_{int},

$$V_t = -\frac{1}{2} f_t \left(\hat{c}^\dagger_{L+1} \hat{c}_{L+2} + \hat{c}^\dagger_{L+2} \hat{c}_{L+1} \right), \qquad f_t = \sin \omega t, \tag{4}$$

$$V_{\text{int}} = U \sum_{j=1}^{2L} n_j n_{j+1}, \tag{5}$$

where ω is the driving frequency, $n_j = c^\dagger_j c_j$ is the particle number operator at the j'th site and U is the interaction strength. Other types of V_t and V_{int} are addressed in the Supplementary Material [14]. The noninteracting case of $U = 0$ was studied in ref. [6].

The number of fermions is conserved and we fix it to be $N = L + 1$. Initially, the fermions fill the left chain, while the right chain is empty:

$$\Psi_0 = \left(\prod_{j=1}^{L+1} c^\dagger_j \right) |\text{vac}\rangle. \tag{6}$$

The state of the system Ψ_t evolves according to the Schrödinger equation $i\partial_t \Psi_t = H_t \Psi_t$.

We focus on a specific observable, the number of fermions in the right chain:

$$N_R = \sum_{j=L+2}^{2L+1} n_j. \tag{7}$$

Its expectation value $\langle N_R \rangle_t = \langle \Psi_t | N_R | \Psi_t \rangle$ is initially zero and grows as a result of particle flow through the QPC.

At large times N_R is expected to fluctuate around its long-time average $\langle N_R \rangle_\infty \equiv \lim\limits_{t \to \infty} t^{-1} \int_0^t dt' \langle N_R \rangle_{t'}$. In the absence of degeneracies in the Floquet spectrum, $\langle N_R \rangle_\infty$ can be computed as

$$\langle N_R \rangle_\infty = \sum_\alpha |\langle \Phi_\alpha | \Psi_0 \rangle|^2 \langle \Phi_\alpha | N_R | \Phi_\alpha \rangle, \tag{8}$$

where Φ_α are the Floquet eigenstates, i.e. eigenstates of the operator of quantum evolution over the driving period $\tau = 2\pi / \omega$.
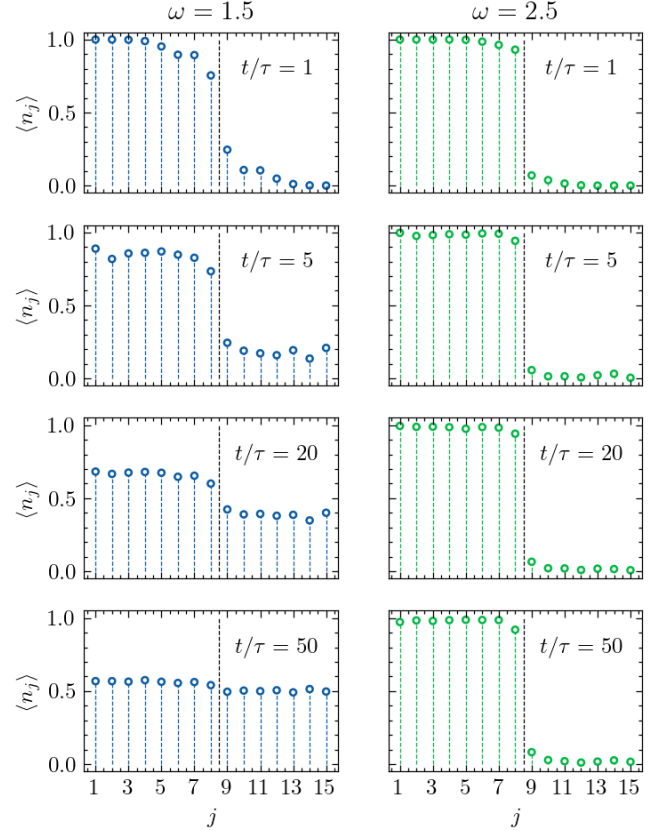

FIG. 2. Evolution of particle density for two driving frequencies. For a frequency below the critical one (left column) particles tend to distribute uniformly over sites. For a frequency above the critical one (right column) the particle imbalance between the chains is retained. Dashed horizontal line delineates two chains.

Results. We use the QuSpin package [15, 16] to numerically solve the Schrödinger equation and compute Floquet spectrum and eigenstates for finite systems of sizes up to $2L + 1 = 15$. We do this for various frequencies. We find qualitative differences in the dynamics and Floquet eigenstates above and below some critical frequency ω_c, see Fig. 3. For not too large interaction strengths $U \lesssim 1$, this critical frequency approximately equals 2, as in the noninteracting case [6].

For frequencies below the critical one the system evolves towards thermalization: particles flow from the left chain to the right one through the QPC and eventually distribute uniformly across both chains, see Fig. 2 and Fig. 3 (a). The equilibrium value $\langle N_R \rangle_\infty$ coincides, up to small finite size corrections, with the value

$$\overline{N}_R = N L / (2L + 1) \tag{9}$$

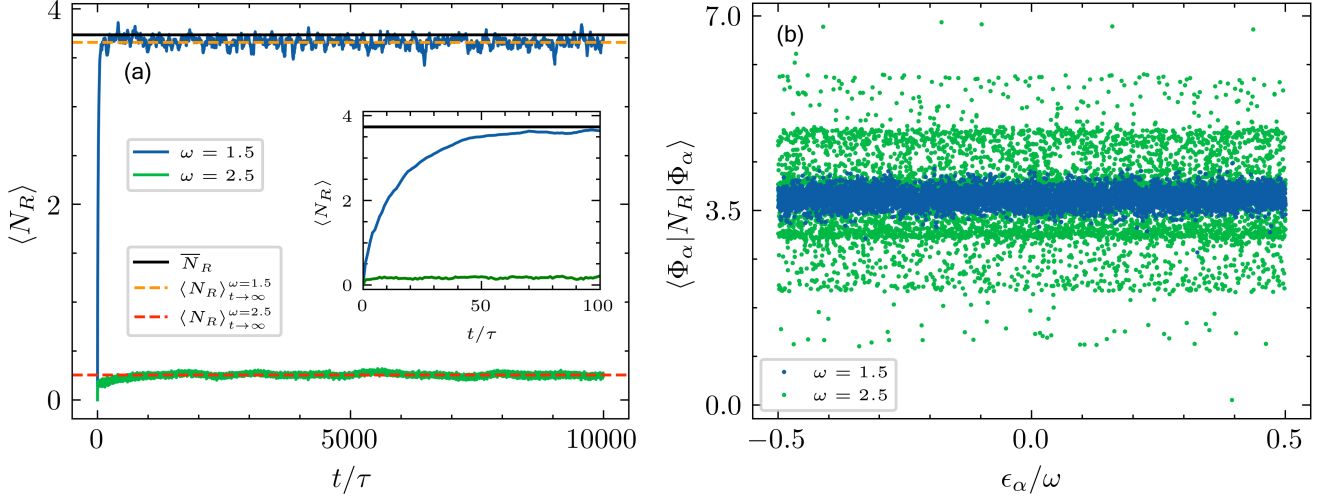obtained for the uniform distribution of particles over the

FIG. 3. (a) The number of particles in the right chain, $\langle N_R \rangle_t$, as a function of time for frequencies below ($\omega = 1.5$) and above ($\omega = 2.5$) the critical frequency. Steady state values computed according to eq. (8) are shown by horizontal dashed lines. The horizontal black line shows the value of N_R corresponding to the uniform distribution of particles over the chains. The interaction strength is $U = 0.5$. The total number of sites and fermions is $2L + 1 = 15$ and $N = 8$, respectively. (b) Diagonal matrix elements of the operator N_R in Floquet basis for different Floquet energies ϵ_α.
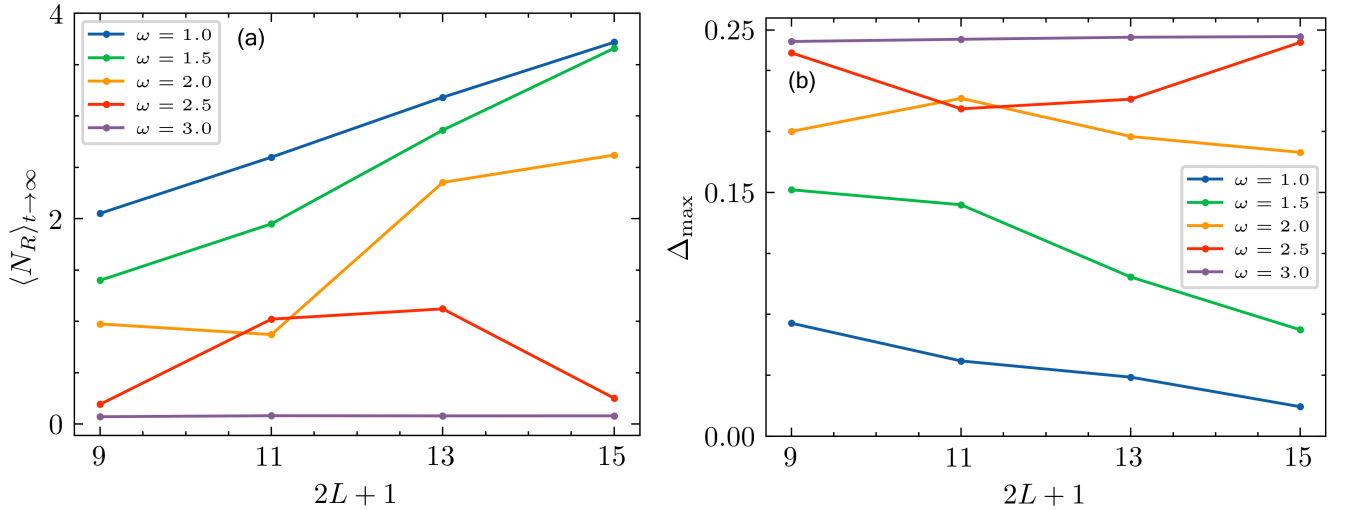

FIG. 4. The scaling with the system size of (a) the steady state value $\langle N_R \rangle_\infty$ and (b) the maximal deviation of the diagonal matrix element $\langle \Phi_\alpha | N_R | \Phi_\alpha \rangle$ from the uniform value $\overline{N}_R$. The interaction strength is $U = 0.5$. One can see the quantitative difference in the scaling behavior for frequencies below and above the critical frequency $\omega_c \simeq 2$.

sites of the system.

In contrast, for frequencies above the critical one the QPC effectively turns insulating: the particles stay in the left chain and never come to the right one. In this case the equilibrium value $\langle N_R \rangle_\infty$ is around zero, as shown in Fig. 2 and Fig. 3 (a).

The diagonal matrix elements $\langle \Phi_\alpha | N_R | \Phi_\alpha \rangle$ of N_R over the Floquet basis is shown in Fig. 3 (b). The patterns below and above the critical frequency are distinctly different. Below the critical frequency the matrix elements tightly concentrate around $\overline{N}_R$, consistent with the Flo-

quet ETH.

In contrast, above the critical frequency matrix elements are scattered over a wide interval, with minimum and maximal instances almost reaching minimal and maximal eigenvalues of N_R, which are 0 and L, respectively.

To check whether our results can be relevant in the thermodynamic limit, we perform a finite size scaling, see Fig. 4. In Fig. 4 (a) the scaling of the equilibrium value $\langle N_R \rangle_\infty$ is shown. One can see that for frequencies below the critical one it scales linearly with the system size, as

expected under the assumption of uniform particle distribution in equilibrium. In contrast, for frequencies above the critical one no growth is observed.

In Fig. 4 (b) the Floquet ETH is tested directly. There we plot the maximal deviation $\Delta_{\max}$ of the diagonal matrix element $\langle \Phi_\alpha | N_R | \Phi_\alpha \rangle$ from the uniform value $\overline{N}_R$ (maximization is performed over all Floquet eigenstates), normalized to the system size:

$$\Delta_{\max} = (2L + 1)^{-1} \max_\alpha \left| \langle \Phi_\alpha | N_R | \Phi_\alpha \rangle - \overline{N}_R \right|. \quad (10)$$

If the Floquet ETH is valid, $\Delta_{\max}$ should decrease with the system size. This is indeed the case for frequencies below the critical one, as can be seen from 4 (b). In contrast, above the critical frequency this figure of merit stays approximately constant, indicting the breakdown of the Floquet ETH.

We have verified that the above qualitative picture is robust with respect to variations of the interaction term V_{int}, as well as the periodic function f_t that modulates the hopping amplitude in the QPC in eq. (4), provided it averages to zero over the period, $\int_0^\tau f_t \, dt = 0$. The results for a number of exemplary models are presented in the Supplement [14].

Discussion and outlook. To summarize, we have demonstrated a nonequilibrium phase transition between thermal and athermal phases in a periodically driven interacting disorder-free quantum many-body system. The system consists of two fermionic chains connected by a driven QPC. The transition occurs upon the variation of the driving frequency. For frequencies below the critical one the QPC is conducting, and the fermions eventually spread homogeneously across the chains, in accordance with the Floquet ETH. For frequencies exceeding the critical frequency, the QPC is insulating, and the initial particle imbalance between the chains remains forever, in stark contrast to the prediction based on the Floquet ETH.

The above frequency dependence of the effect sharply distinguishes it from other known types of the Floquet thermalization breakdown. In particular, in non-generic Floquet systems featuring integrability, exact quantum many-body scars or Hilbert space fragmentation, the violation of the Floquet ETH and the thermalization breakdown typically take place for arbitrary driving frequencies, and athermal eigenstates often are independent on the frequency [17–23]. Alternatively, the breakdown or slowdown of thermalization can occur for a discrete set of frequencies in such systems [24–31]. A completely different frequency dependence of the Floquet ETH violation reported here may indicate a distinct origin of this violation – a question left for further studies.

It should be emphasized that the thermalization breakdown reported here can not be explained by the Floquet prethermalization [32–36]. The latter phenomenon implies the thermalization slowdown at large frequencies, with the thermalization time depending exponentially on the frequency. If the system under study exhibited "mere" prethermalization, the particle imbalance between the chains would be eventually washed out. We know that this is not the case, since in finite systems under study we have access to arbitrary long times, as well as to the infinite-time averages (8). Furthermore, the critical frequency is not, in fact, large enough for the prethermalization mechanism to be effective, as we demonstrate in the Supplement [14].

An intriguing question for further studies concerns the scope of the reported effect. While we have demonstrated its robustness in one-dimensional geometry, our numerical tests do not extend to higher dimensions. It is not uncommon when exotic out-of-equilibrium phenomena in one dimension have no counterparts in higher dimensions [37–42]. It is therefore reasonable to ask whether the reported type of the Floquet thermalization breakdown extends beyond one-dimensional geometry. We note that this question, while challenging for numerical exploration, can perhaps be addressed with the state-of-the-art quantum simulators with planar arrangement of qubits [43–47].

As a word of caution, we note that, in the case of non-interacting fermions, dissipation (caused e.g. by phonon-fermion interactions) destroys the phase transition and makes the QPC conducting at any frequency [48]. Likely it will have the same effect in the interacting case. This should be accounted for while conceiving experimental tests of the effect.

———————

[1] Yuli V Nazarov and Yaroslav M Blanter, *Quantum transport: introduction to nanoscience* (Cambridge university press, 2009).

[2] Gloria Platero and Ramón Aguado, "Photon-assisted transport in semiconductor nanostructures," Physics Reports **395**, 1–157 (2004).

[3] Sigmund Kohler, Jorg Lehmann, and Peter Hanggi, "Driven quantum transport on the nanoscale," Physics Reports **406**, 379–443 (2005).

[4] Dmitry A Ryndyk *et al.*, "Theory of quantum transport at nanoscale," Springer Series in Solid-State Sciences **184**, 9 (2016).

[5] Gabriel T. Landi, Dario Poletti, and Gernot Schaller, "Nonequilibrium boundary-driven quantum systems: Models, methods, and properties," Rev. Mod. Phys. **94**,

045006 (2022).

[6] Oleksandr Gamayun, Artur Slobodeniuk, Jean-Sébastien Caux, and Oleg Lychkovskiy, "Nonequilibrium phase transition in transport through a driven quantum point contact," Physical Review B **103**, L041405 (2021).

[7] Achilleas Lazarides, Arnab Das, and Roderich Moessner, "Equilibrium states of generic quantum systems subject to periodic driving," Phys. Rev. E **90**, 012110 (2014).

[8] Luca D'Alessio and Marcos Rigol, "Long-time behavior of isolated periodically driven interacting lattice systems," Phys. Rev. X **4**, 041048 (2014).

[9] Karthik Seetharam, Paraj Titum, Michael Kolodrubetz, and Gil Refael, "Absence of thermalization in finite isolated interacting floquet systems," Phys. Rev. B **97**, 014311 (2018).

[10] Bingtian Ye, Francisco Machado, Christopher David White, Roger S. K. Mong, and Norman Y. Yao, "Emergent hydrodynamics in nonequilibrium quantum systems," Phys. Rev. Lett. **125**, 030601 (2020).

[11] Andrea Pizzi, Daniel Malz, Giuseppe De Tomasi, Johannes Knolle, and Andreas Nunnenkamp, "Time crystallinity and finite-size effects in clean floquet systems," Phys. Rev. B **102**, 214207 (2020).

[12] Tatsuhiko N. Ikeda and Anatoli Polkovnikov, "Fermi's golden rule for heating in strongly driven floquet systems," Phys. Rev. B **104**, 134308 (2021).

[13] Alan Morningstar, David A. Huse, and Vedika Khemani, "Universality classes of thermalization for mesoscopic floquet systems," Phys. Rev. B **108**, 174303 (2023).

[14] See the Supplemental Material for results on various types of QPCs and interparticle interactions, as well as for an estimate of the prethermalization timescale.

[15] Phillip Weinberg and Marin Bukov, "QuSpin: a Python package for dynamics and exact diagonalisation of quantum many body systems part I: spin chains," SciPost Phys. **2**, 003 (2017).

[16] Phillip Weinberg and Marin Bukov, "QuSpin: a Python package for dynamics and exact diagonalisation of quantum many body systems. Part II: bosons, fermions and higher spins," SciPost Phys. **7**, 020 (2019).

[17] Vladimir Gritsev and Anatoli Polkovnikov, "Integrable Floquet dynamics," SciPost Phys. **2**, 021 (2017).

[18] Kaoru Mizuta, Kazuaki Takasan, and Norio Kawakami, "Exact floquet quantum many-body scars under rydberg blockade," Phys. Rev. Res. **2**, 033284 (2020).

[19] H. Yarloo, A. Emami Kopaei, and A. Langari, "Homogeneous floquet time crystal from weak ergodicity breaking," Phys. Rev. B **102**, 224309 (2020).

[20] Vedika Khemani, Michael Hermele, and Rahul Nandkishore, "Localization from hilbert space shattering: From theory to physical realizations," Phys. Rev. B **101**, 174204 (2020).

[21] Bhaskar Mukherjee, Sourav Nandy, Arnab Sen, Diptiman Sen, and K. Sengupta, "Collapse and revival of quantum many-body scars via floquet engineering," Phys. Rev. B **101**, 245107 (2020).

[22] Sanjay Moudgalya, B Andrei Bernevig, and Nicolas Regnault, "Quantum many-body scars and hilbert space fragmentation: a review of exact results," Reports on Progress in Physics **85**, 086501 (2022).

[23] Alexander Teretenkov and Oleg Lychkovskiy, "Duality between open systems and closed bilayer systems, and thermofield double states as quantum many-body scars," arXiv preprint arXiv:2304.03155 (2023).

[24] Arnab Das, "Exotic freezing of response in a quantum many-body system," Phys. Rev. B **82**, 172402 (2010).

[25] Sirshendu Bhattacharyya, Arnab Das, and Subinay Dasgupta, "Transverse ising chain under periodic instantaneous quenches: Dynamical many-body freezing and emergence of slow solitary oscillations," Phys. Rev. B **86**, 054410 (2012).

[26] Asmi Haldar, Roderich Moessner, and Arnab Das, "Onset of floquet thermalization," Phys. Rev. B **97**, 245122 (2018).

[27] Asmi Haldar, Diptiman Sen, Roderich Moessner, and Arnab Das, "Dynamical freezing and scar points in strongly driven floquet matter: Resonance vs emergent conservation laws," Phys. Rev. X **11**, 021008 (2021).

[28] Christoph Fleckenstein and Marin Bukov, "Prethermalization and thermalization in periodically driven many-body systems away from the high-frequency limit," Phys. Rev. B **103**, L140302 (2021).

[29] Sho Sugiura, Tomotaka Kuwahara, and Keiji Saito, "Many-body scar state intrinsic to periodically driven system," Phys. Rev. Res. **3**, L012010 (2021).

[30] Sreemayee Aditya and Diptiman Sen, "Dynamical localization and slow thermalization in a class of disorder-free periodically driven one-dimensional interacting systems," SciPost Phys. Core **6**, 083 (2023).

[31] Somsubhra Ghosh, Indranil Paul, and K. Sengupta, "Prethermal fragmentation in a periodically driven fermionic chain," Phys. Rev. Lett. **130**, 120401 (2023).

[32] Dmitry A. Abanin, Wojciech De Roeck, and Francois Huveneers, "Exponentially slow heating in periodically driven many-body systems," Phys. Rev. Lett. **115**, 256803 (2015).

[33] Takashi Mori, Tomotaka Kuwahara, and Keiji Saito, "Rigorous bound on energy absorption and generic relaxation in periodically driven quantum systems," Phys. Rev. Lett. **116**, 120401 (2016).

[34] Antonio Rubio-Abadal, Matteo Ippoliti, Simon Hollerith, David Wei, Jun Rui, S. L. Sondhi, Vedika Khemani, Christian Gross, and Immanuel Bloch, "Floquet prethermalization in a bose-hubbard system," Phys. Rev. X **10**, 021044 (2020).

[35] William Beatrez, Otto Janes, Amala Akkiraju, Arjun Pillai, Alexander Oddo, Paul Reshetikhin, Emanuel Druga, Maxwell McAllister, Mark Elo, Benjamin Gilbert, Dieter Suter, and Ashok Ajoy, "Floquet prethermalization with lifetime exceeding 90 s in a bulk hyperpolarized solid," Phys. Rev. Lett. **127**, 170603 (2021).

[36] Wen Wei Ho, Takashi Mori, Dmitry A. Abanin, and Emanuele G. Dalla Torre, "Quantum and classical floquet prethermalization," Annals of Physics **454**, 169297 (2023).

[37] M. B. Zvonarev, V. V. Cheianov, and T. Giamarchi, "Spin dynamics in a one-dimensional ferromagnetic bose gas," Phys. Rev. Lett. **99**, 240404 (2007).

[38] Michael Knap, Charles J. M. Mathy, Martin Ganahl, Mikhail B. Zvonarev, and Eugene Demler, "Quantum flutter: Signatures and robustness," Phys. Rev. Lett. **112**, 015302 (2014).

[39] E. Burovski, V. Cheianov, O. Gamayun, and O. Lychkovskiy, "Momentum relaxation of a mobile impurity in a one-dimensional quantum gas," Phys. Rev. A **89**, 041601 (2014).

[40] O. Lychkovskiy, "Perpetual motion of a mobile impurity in a one-dimensional quantum gas," Phys. Rev. A **89**,

033619 (2014).

[41] O. Lychkovskiy, "Perpetual motion and driven dynamics of a mobile impurity in a quantum fluid," Phys. Rev. A **91**, 040101(R) (2015).

[42] B. Bertini, F. Heidrich-Meisner, C. Karrasch, T. Prosen, R. Steinigeweg, and M. Znidaric, "Finite-temperature transport in one-dimensional quantum lattice models," Rev. Mod. Phys. **93**, 025003 (2021).

[43] Frank Arute, Kunal Arya, Ryan Babbush, Dave Bacon, Joseph C Bardin, Rami Barends, Rupak Biswas, Sergio Boixo, Fernando GSL Brandao, David A Buell, *et al.*, "Quantum supremacy using a programmable superconducting processor," Nature **574**, 505–510 (2019).

[44] Ming Gong, Shiyu Wang, Chen Zha, Ming-Cheng Chen, He-Liang Huang, Yulin Wu, Qingling Zhu, Youwei Zhao, Shaowei Li, Shaojun Guo, Haoran Qian, Yangsen Ye, Fusheng Chen, Chong Ying, Jiale Yu, Daojin Fan, Dachao Wu, Hong Su, Hui Deng, Hao Rong, Kaili Zhang, Sirui Cao, Jin Lin, Yu Xu, Lihua Sun, Cheng Guo, Na Li, Futian Liang, V. M. Bastidas, Kae Nemoto, W. J. Munro, Yong-Heng Huo, Chao-Yang Lu, Cheng-Zhi Peng, Xiaobo Zhu, and Jian-Wei Pan, "Quantum walks on a programmable two-dimensional 62-qubit superconducting processor," Science **372**, 948–952 (2021).

[45] Sepehr Ebadi, Tout T. Wang, Harry Levine, Alexander Keesling, Giulia Semeghini, Ahmed Omran, Daniel Bluvstein, Rhine Samajdar, Hannes Pichler, Wen Wei Ho, *et al.*, "Quantum phases of matter on a 256-atom programmable quantum simulator," Nature **595**, 227–232 (2021).

[46] Pascal Scholl, Michael Schuler, Hayden Williams, Astrid Eberharter, Daniel Barredo, Konrad Schymik, Vincent Lienhard, Louis-Paul Henry, Thomas Boulier, Robert Blumel, *et al.*, "Quantum simulation of 2d ising models using rydberg atoms," Nature **595**, 233–238 (2021).

[47] Vincent Lienhard, Sylvain de Leseleuc, Daniel Barredo, Thierry Lahaye, and Antoine Browaeys, "Observing a many-body quantum transition using a 51-atom quantum simulator," Nature **573**, 569–573 (2018).

[48] Igor Ermakov and Oleg Lychkovskiy, "Effect of dephasing on the current through a periodically driven quantum point contact," JETP Letters **119**, 40–45 (2024).

Supplementary material

to the Letter
"Fermionic transport through a driven quantum point contact:
breakdown of Floquet thermalization beyond a critical driving frequency"
by Ivan V. Dudinets and Oleg Lychkovskiy.

S1. Various driving protocols

Here we present results for various driving protocols f_t in eq. (4). The protocols under study are shown in Fig. S1. The results are shown in Figs. S2— S5. One can see that they are qualitatively similar to the results reported in the main text.
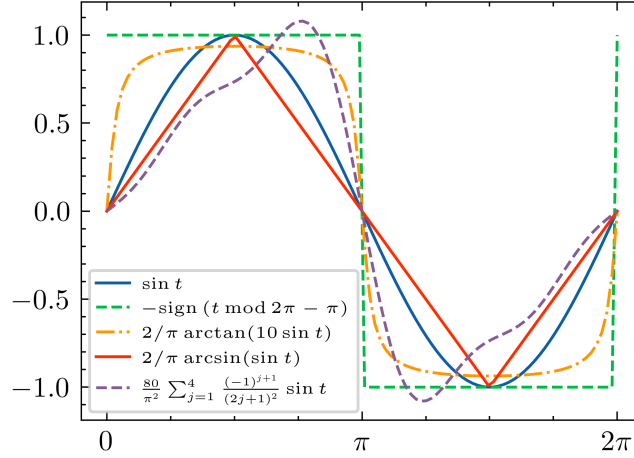

FIG. S1. Plot of the driving protocols, f_t, as a function of time. Here the driving frequency is set to 1.

S2. A QPC with on-site potential

It was found in ref. [6] that, in the noninteracting case, an alternating on-site potential within the QPC typically destroys the effect and ensures the current flow at any frequency. However, a notable exception was found for the QPC term V_t given by

$$V_t = -\frac{1}{2} \begin{pmatrix} \hat{c}^\dagger_{L+1} & \hat{c}_{L+2} \end{pmatrix} \begin{pmatrix} g_t & f_t \\ f_t & -g_t \end{pmatrix} \begin{pmatrix} \hat{c}^\dagger_{L+1} \\ \hat{c}_{L+2} \end{pmatrix}. \tag{S1}$$

with the tunneling amplitude $f_t = \sin(\omega t)$ and on-site potential $g_t = \sin(\omega t)$. We have found the same qualitative picture in the interacting case. In particular, the current halts completely for the above V_t, as shown in Fig. S6.

S3. Various interaction terms

We have verified that the physical picture remains the same for various types of interaction terms. As an illustration, we show in Fig. S7 the results for

$$V_{\mathrm{int}} = U \sum_{j=1}^{2L} n_j n_{j+1} + U' \sum_{j=1}^{2L-1} n_j n_{j+2}, \tag{S2}$$

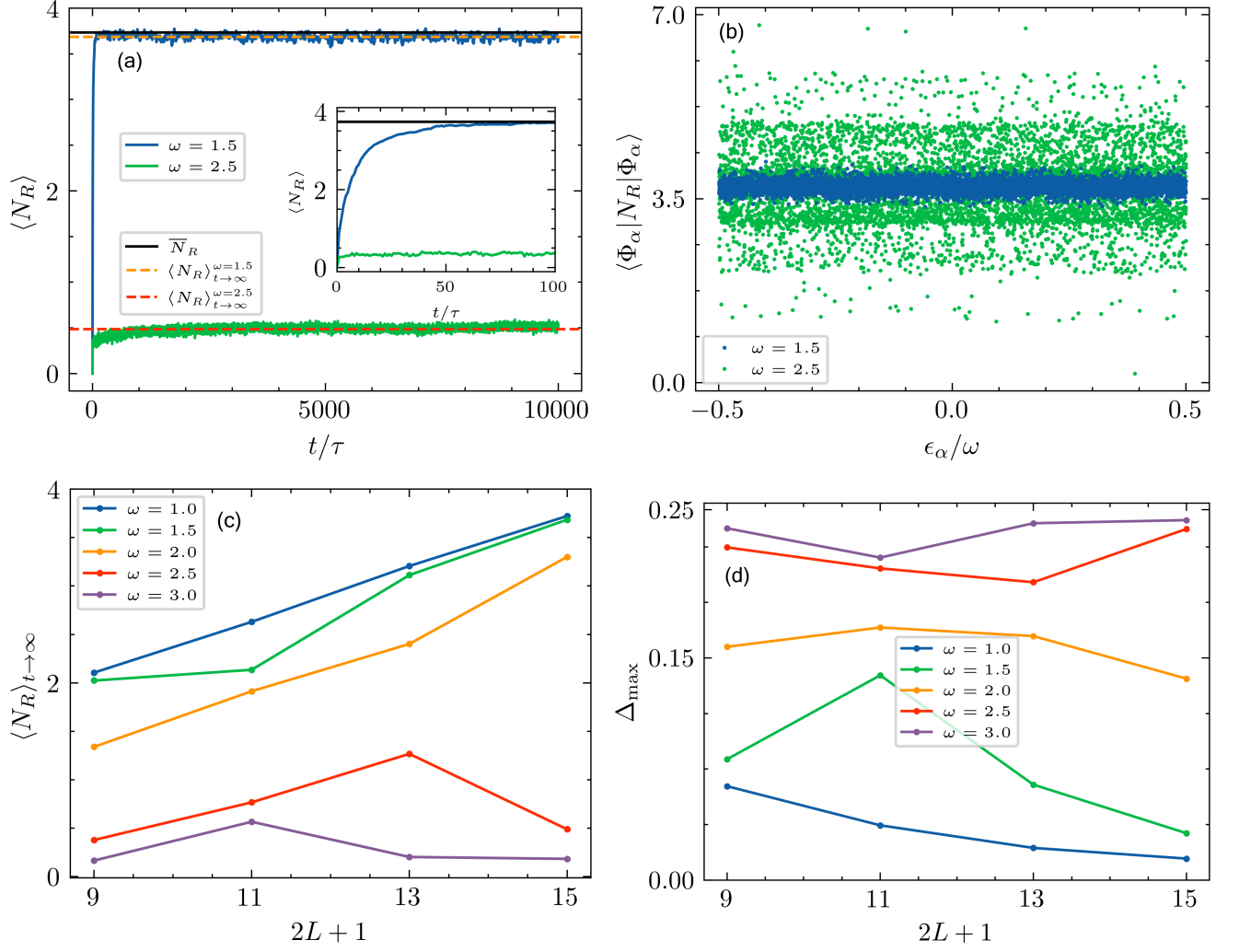where U and U' are two interaction constants.

FIG. S2. Results for the driving protocol $f_t = -\text{sign}\left(t \bmod \frac{2\pi}{\omega} - \frac{\pi}{\omega}\right)$. The interaction strength is $U = 0.5$. (a) The number of particles in the right chain, $\langle N_R \rangle_t$, as a function of time for frequencies below ($\omega = 1.5$) and above ($\omega = 2.5$) the critical frequency $\omega_c \simeq 2$. Horizontal dashed lines correspond to steady state values computed according to eq. (8). The horizontal black line shows the value of N_R corresponding to the uniform distribution of particles over the chains. (b) Diagonal matrix elements of the operator N_R in Floquet basis for different Floquet energies ϵ_α. In Figs. (a) and (b) the system comprises $2L + 1 = 15$ sites and $N = 8$ fermions. (c) The steady state value $\langle N_R \rangle_\infty$ for the system of various sizes. (d) The maximal deviation of the diagonal matrix element $\langle \Phi_\alpha | N_R | \Phi_\alpha \rangle$ from the uniform value $\overline{N}_R$.
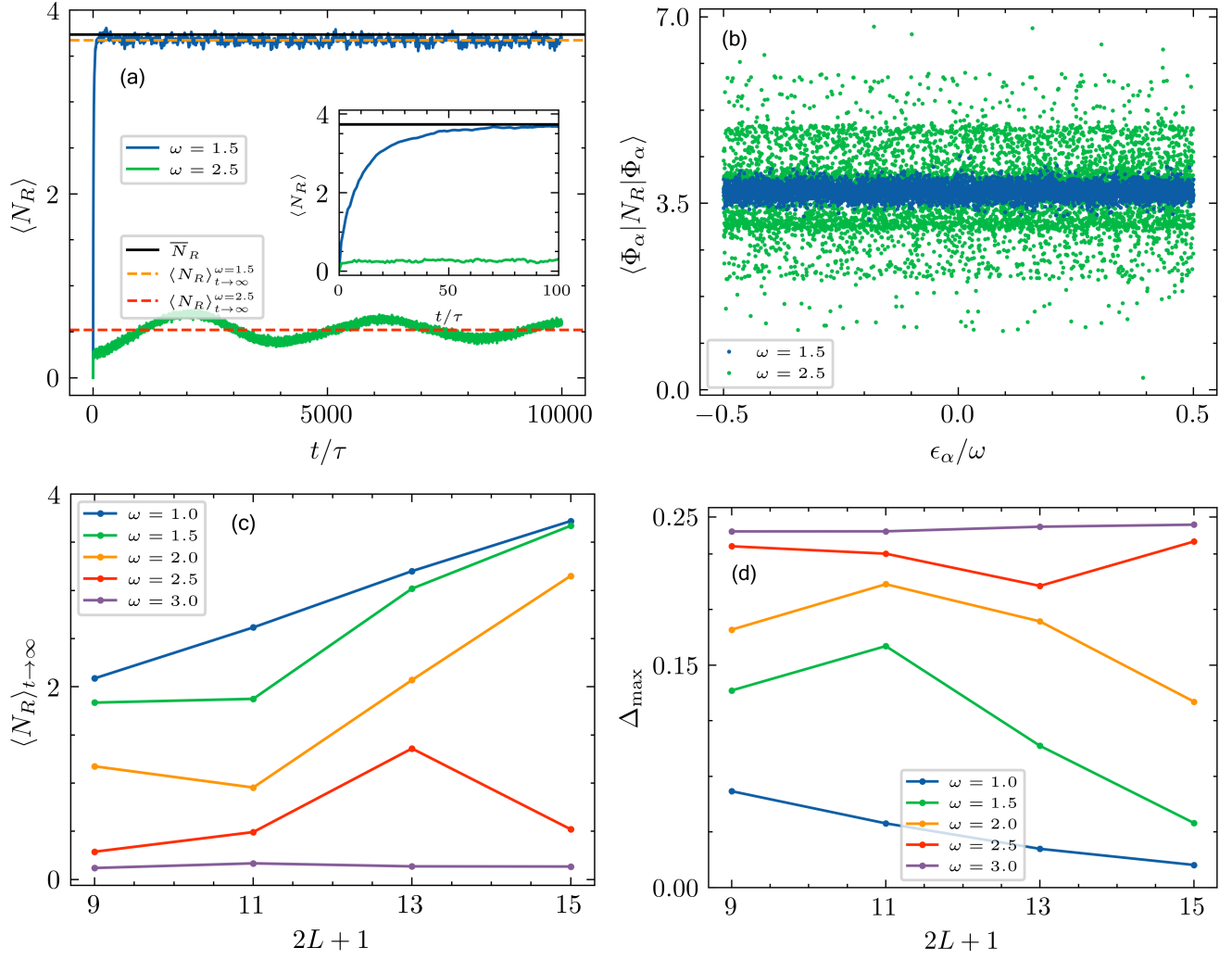
FIG. S3. The same as in Fig. S2 except for the driving protocol $f_t = \frac{2}{\pi}\arctan\left(\sin 10\,\omega t\right)$.
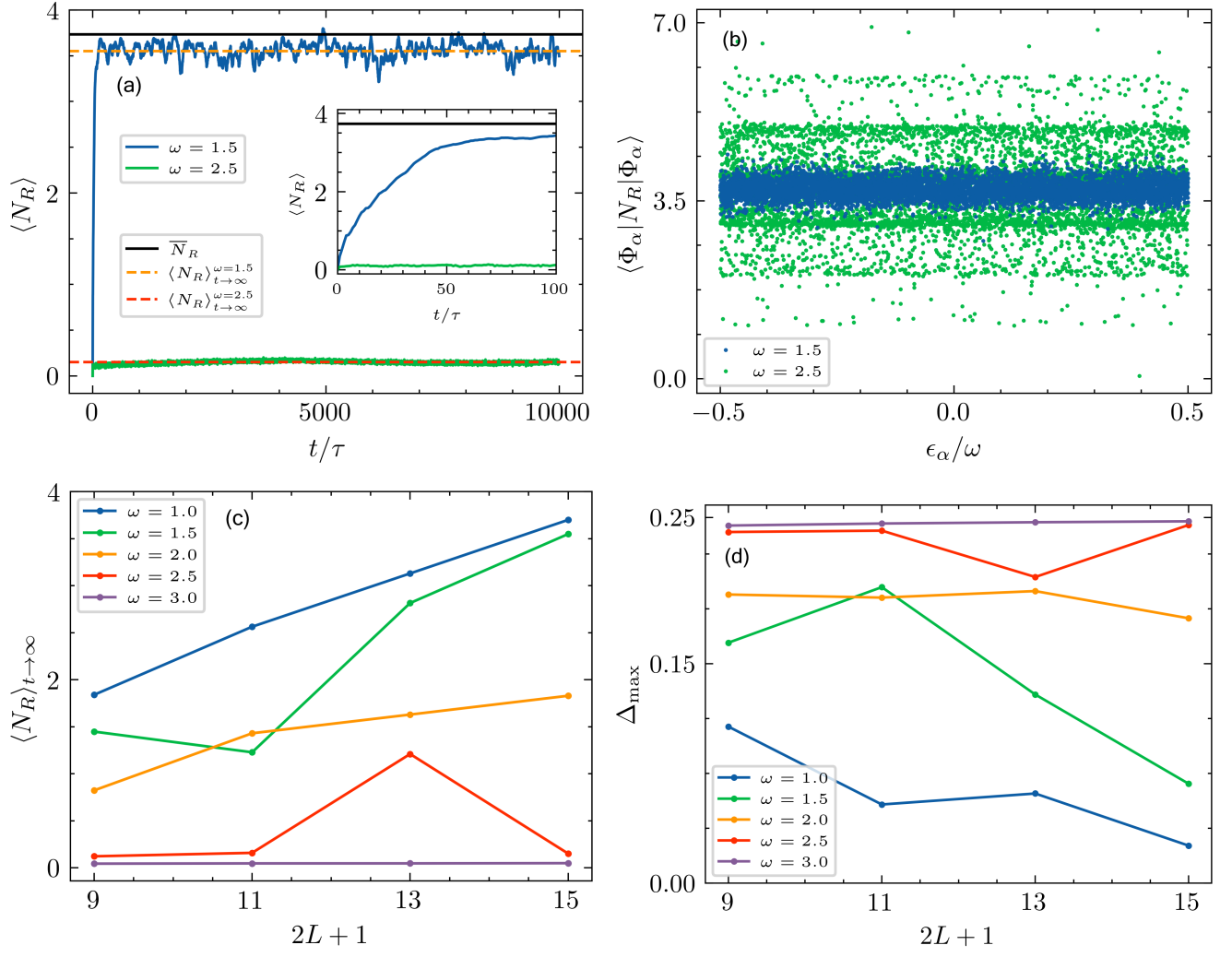
FIG. S4. The same as in Fig. S2 except for the driving protocol $f_t = \frac{2}{\pi} \arcsin{(\sin \omega t)}$.
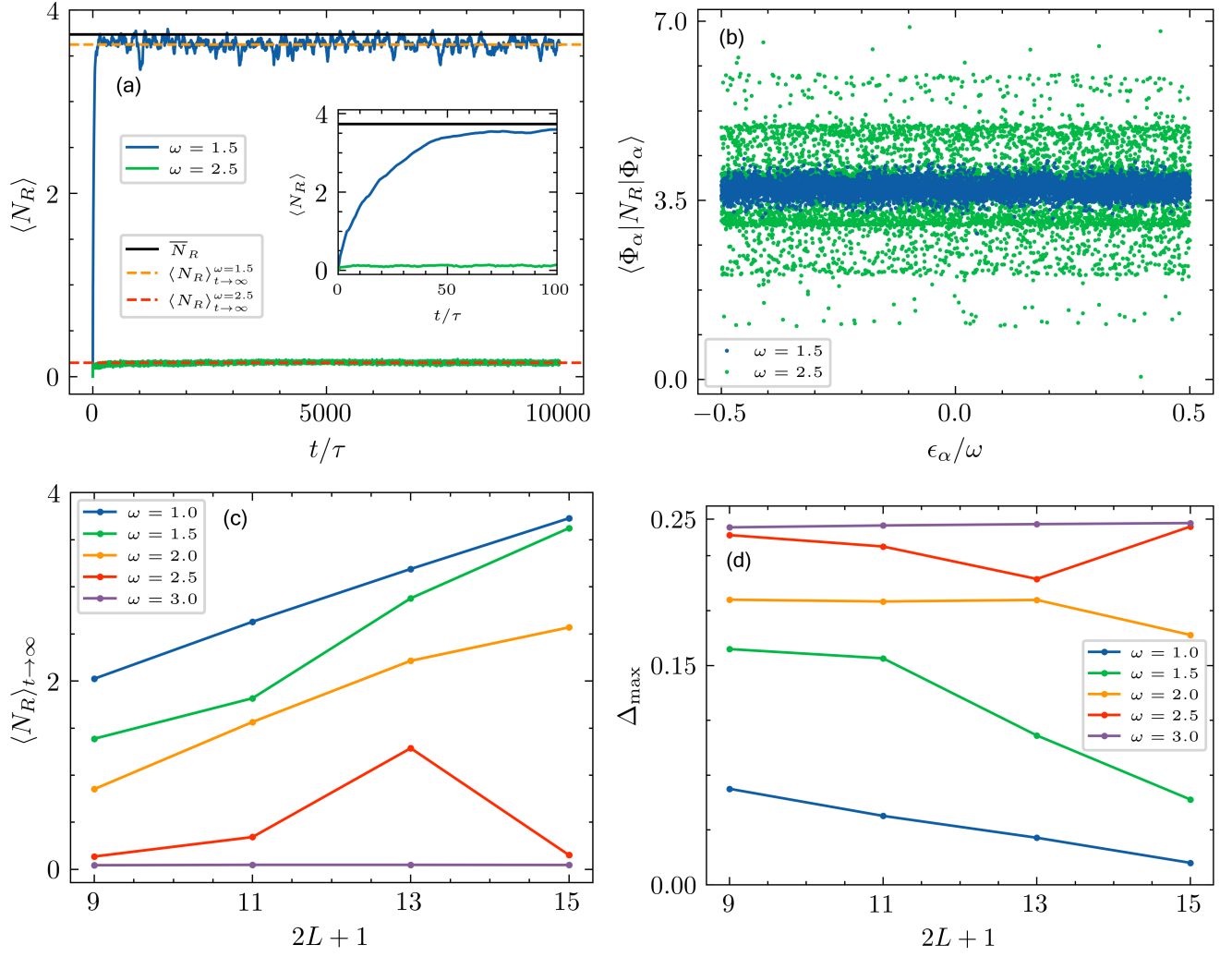
FIG. S5. The same as in Fig. S2 except for the driving protocol $f_t = \frac{80}{\pi^2} \sum_{j=1}^{4} \frac{(-1)^{j+1}}{(2j+1)^2} \sin \omega t$.
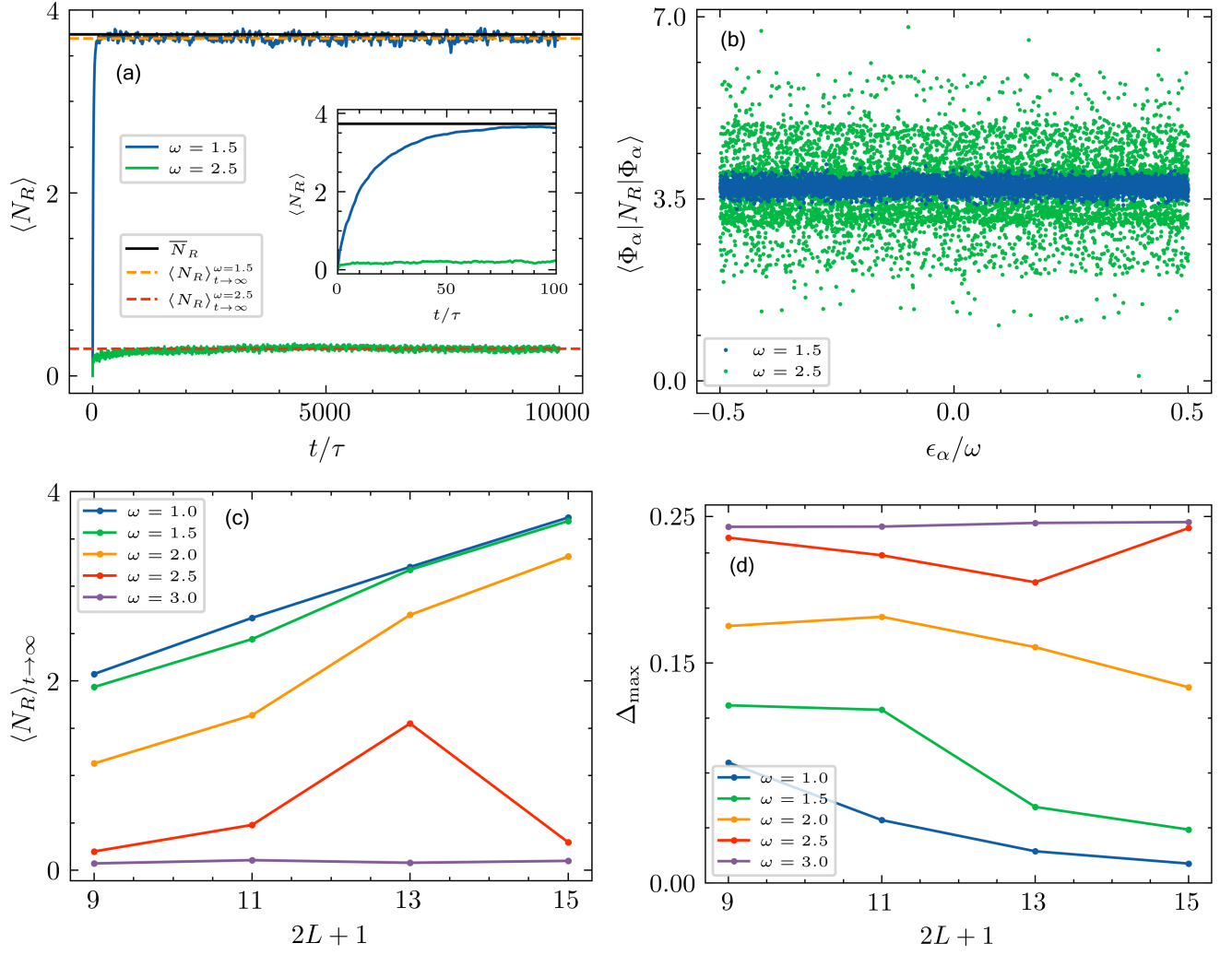
FIG. S6. The same as in Fig. S2 except for the QPC Hamiltonian V_t given by eq. (S1) with the tunneling amplitude $f_t = \sin \omega t$ and on-site potential $g_t = \sin \omega t$.
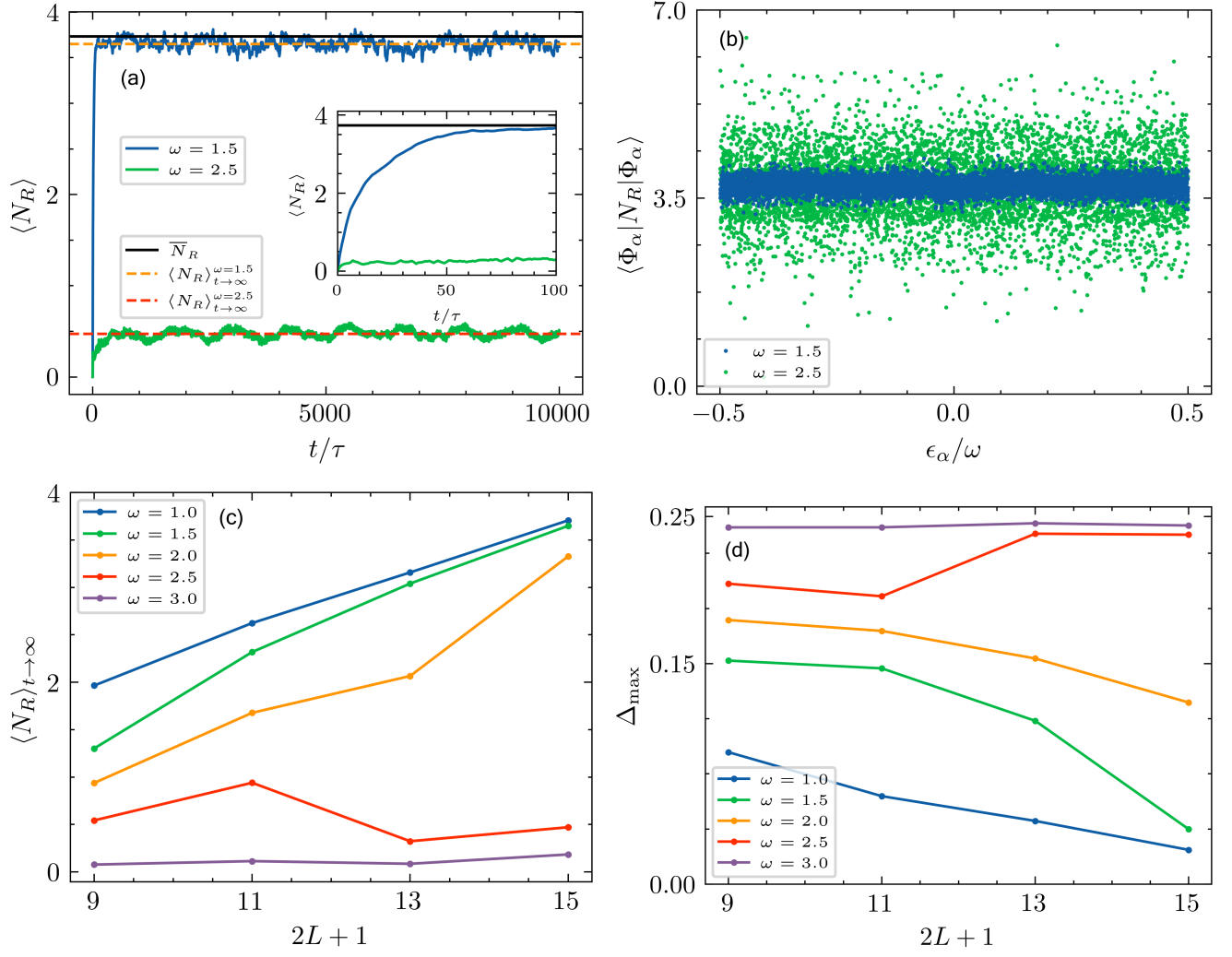
FIG. S7. The same as in Fig. S2 except for the driving protocol $f_t = \sin \omega t$ and the interaction term V_{int} given by eq. (S2) with $U = U' = 0.5$.

S4. Estimate of the prethermalization time and energy scales

A conservative estimate Λ of the prethermalization energy scale is obtained as the sum of operator norms of Hamiltonian terms with a support covering a fixed site [36]. For our system (1)-(5) this implies $\Lambda = 1 + 2U$.

The ratio of frequency-dependent thermalization timescales $\tau_{\text{th}}(\omega)$ for two different frequencies is estimated as $\tau_{\text{th}}(\omega_2)/\tau_{\text{th}}(\omega_1) \sim \exp\left((\omega_2 - \omega_1)/\Lambda\right)$. For $\omega_1 = 1.5$, $\omega_2 = 2.5$ and $U = 0.5$ this estimate reads $\tau_{\text{th}}(\omega_2)/\tau_{\text{th}}(\omega_1) \sim \sqrt{e} \simeq 1.6$. Thus the prethermalization timescales for these two frequencies should be of the same order of magnitude. However, we clearly observe thermalization at the frequency ω_1, with $\tau_{\text{th}}(\omega_1) \sim 10$, while no thermalization is observed at the frequency ω_2 up to times $\sim 1000\,\tau_{\text{th}}(\omega_1)$. This argument confirms that the observed lack of thermalization can not be explained by "mere" prethermalization.